

## SCATTERING PARAMETERS OF SEMICONDUCTOR MICROSTRIP LINE UNDER LASER SPOT ILLUMINATION

Yasushi Horii

Faculty of Informatics, Kansai University

2-1-1 Ryozenji-cho, Takatsuki-shi, Osaka 569-11, Japan.

Makoto Tsutsumi

Faculty of Engineering and Design, Kyoto Institute of Technology

Matsugasaki, Sakyo-ku, Kyoto 606, Japan.

### Abstract

Scattering parameters of an optically controlled microstrip gap fabricated on the semiconductor substrate have been analyzed theoretically using the frequency-dependent finite-difference time-domain method.

The transmission characteristics of interest have been shown as a function of arbitrary position of laser spot around an air gap. The results have been demonstrated experimentally using microstrip line with silicon substrate and semiconductor laser. And, it is also reported that the high-powered illumination of laser spot develops non-dispersive characteristics of  $S_{21}$  for the wide frequency range.

### 1. Introduction

When a semiconductor is illuminated with a laser which has a photon energy greater than its band gap, electron-hole pairs, called "plasma", are induced near the surface of the semiconductor, and cause a change of its complex permittivity<sup>[1]</sup>. This makes it possible to control the propagation characteristics of microwaves traveling in the semiconductor. As an application of this phenomenon, an optically controlled gap fabricated on a semiconductor microstrip line is of interest because of its possibility of high speed switching of microwaves and picosecond microwave generation.

In this paper, we have demonstrated in detail the scattering parameters of such a line, both theoretically and experimentally, taking the position and the diameter of laser spot as a parameter<sup>[2]</sup>. For the theoretical analysis, the frequency-dependent finite-difference time-domain method ( (FD)<sup>2</sup>TD method ) was adopted<sup>[3]</sup>.

### 2. Theoretical Analysis

#### 2.1 Analyzed Model

Figure 1 shows an illustration of a microstrip line with an optically controlled gap on a semiconductor substrate surface using a photo-induced semiconductor plasma. Microstrip line with the width  $w = 1.0\text{mm}$  and having zero thickness, is assumed to be made of a perfect conductor. A gap with the width  $G_w = 0.5\text{mm}$  is given on this strip. Silicon substrate with the thickness  $h = 0.4\text{mm}$  and the relative permittivity  $\epsilon_s = 11.8$  is adopted. The density of plasma induced by the overhead laser illumination is defined as:

$$n_p(x, y, z) = n_p(x_0, y_0, z_0) e^{-\frac{1}{R^2}[(x-x_0)^2 + (y-y_0)^2]} e^{-\frac{1}{i_p}|z-z_0|} \quad (1)$$

where,  $2R$  = diameter of the laser spot, and

$n_p(x_0, y_0, z_0)$  = surface plasma density at the center of the laser spot.

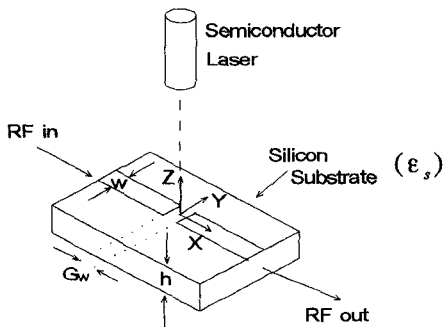


Fig.1 Illustration of the analyzed model.

## 2.2 $(FD)^2TD$ method

The  $(FD)^2TD$  method is capable to express the macroscopic transient electromagnetic interactions with three-dimensional geometry over a large frequency range. In case of dispersive material like a semiconductor plasma, the constitutive equation expressed in the frequency domain is to be transformed into the time domain using the Fourier transformation theory.

Originally, the complex permittivity of plasma is written as<sup>[1]</sup>:

$$\epsilon(\omega) = \epsilon_0 \{ \epsilon_s + \chi_e(\omega) + \chi_h(\omega) \} \quad (2)$$

$$\chi_i(\omega) = \frac{\omega_{pi}^2}{\omega(j\nu_i - \omega)} \quad (i = e, h) \quad (3)$$

$$\omega_{pi}^2 = \frac{n_p e^2}{\epsilon_0 m_i} \quad (4)$$

where,  $\chi_i(\omega)$ : electric susceptibility

$\epsilon_0$ : permittivity of free space

$\epsilon_s$ : relative permittivity for  $\omega \rightarrow 0$

$\omega_{pi}$ : plasma frequency  $e$ : electron charge

$\omega$ : microwave frequency  $m_i$ : effective mass

$\nu_i$ : collision frequency  $n_p$ : plasma density

The constitutive relation in the frequency domain is given as:

$$E_y^{n+1}(i, j + \frac{1}{2}, k) = \frac{\epsilon_s + \Delta\chi_{0e} + \Delta\chi_{0h}}{\epsilon_0 + \chi_{0e} + \chi_{0h}} E_y^n(i, j + \frac{1}{2}, k) + \frac{1}{\epsilon_s + \chi_{0e} + \chi_{0h}} \left\{ \sum_{m=1}^{n-1} E_y^{n-m}(i, j + \frac{1}{2}, k) (\Delta\chi_{0e} + \Delta\chi_{0h}) \right\} + \frac{\Delta t}{\epsilon_s + \chi_{0e} + \chi_{0h}} \left\{ \frac{H_z^{n+\frac{1}{2}}(i + \frac{1}{2}, j + \frac{1}{2}, k) - H_z^{n+\frac{1}{2}}(i - \frac{1}{2}, j + \frac{1}{2}, k)}{\Delta x} - \frac{H_x^{n+\frac{1}{2}}(i, j + \frac{1}{2}, k + \frac{1}{2}) - H_x^{n+\frac{1}{2}}(i, j + \frac{1}{2}, k - \frac{1}{2})}{\Delta z} \right\} \quad (9)$$

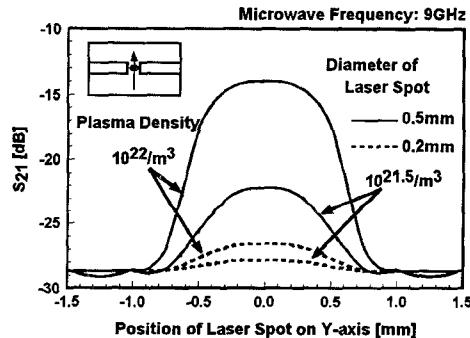


Fig.2 The transmission characteristics of  $S_{21}$  when the laser spot passes through Y-axis.

$$\mathbf{D}(\omega) = \epsilon(\omega) \mathbf{E}(\omega)$$

$$= \epsilon_0 (\epsilon_s + \chi_e(\omega) + \chi_h(\omega)) \mathbf{E}(\omega) \quad (5)$$

By the Fourier transformation of the equation (5), the time domain formulation can be derived as follows<sup>[4]</sup>:

$$\mathbf{D}(t) = \epsilon_s \epsilon_0 \mathbf{E}(t) + \epsilon_0 \int_0^t \mathbf{E}(t - \tau) (\chi_e(\tau) + \chi_h(\tau)) d\tau \quad (6)$$

$$\chi_i(t) = \frac{\omega_{pi}^2}{\nu_i} (1 - e^{-\nu_i t}) U(t) \quad (7)$$

where  $U(t)$  denotes the unit step function. Here, we let  $t = n\Delta t$ , and the equation (6) can be quantized as

$$\mathbf{D}^n = \epsilon_s \epsilon_0 \mathbf{E}^n + \epsilon_0 \sum_{m=0}^{n-1} \mathbf{E}^{n-m} \int_{m\Delta t}^{(m+1)\Delta t} (\chi_e(\tau) + \chi_h(\tau)) d\tau \quad (8)$$

Introducing the equation (8) into the quantized expression of Maxwell's equations, all the field components can be formulated. For instance, the equation (9) is the quantized formulation of  $E_y$ .

The field components are arranged on Yee's mesh<sup>[5]</sup>, consisting of 310, 80 and 20 spatial cells in x, y and z directions. The size of smallest cell are  $\Delta x = \Delta y = 0.05$  mm and  $\Delta z = 0.025$  mm. The time step is  $\Delta t = 6.75 \times 10^{-14}$  (s). Calculations are made for a normally incident plane wave with a time behavior given by the derivative of a Gaussian pulse. To eliminate unwanted reflections, boundary walls are taken as absorbing type<sup>[6]</sup>.

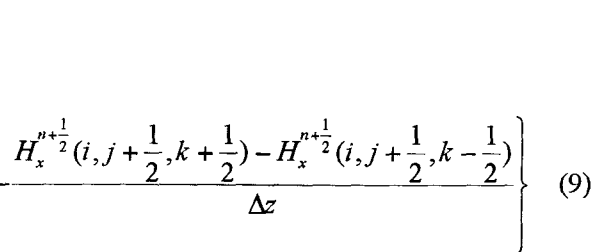


Fig.3 The transmission characteristics of  $S_{21}$  when the laser spot passes through X-axis.

### 3. Theoretical Results

#### 3.1 Scanning of the Laser Spot around the Gap

Transmission characteristics  $S_{21}$  of the line are calculated here when the laser spot with the diameter  $2R = 0.2\text{mm}$  or  $0.5\text{mm}$  scans around the gap. The microwave frequency is fixed at 9GHz and the thickness of plasma is assumed to be  $t_p = 0.025\text{mm}$ . Here, Y defines an axis in the horizontal plane which passes the center of the gap and keeps the equal distance between the strips. And, X is orthogonal to Y and also passes the center of the gap.

Figure 2 shows the value of  $S_{21}$  when the laser passes through Y axis. It is apparent from the figure that the variation in  $S_{21}$  becomes larger when the plasma density is higher or the diameter of the laser spot is bigger. Further, the maximum value of  $S_{21}$ ,

$S_{21\text{max}}$ , is obtained when the laser spot is just at the center of the gap.

In figure 3, the characteristics of  $S_{21}$  is presented when the laser spot moves in the X-direction. These results imply that the  $S_{21}$  has a particular feature in relation to the diameter of laser spot. In the case of  $2R = 0.5\text{mm}$ , the  $S_{21}$  becomes maximum at  $x = 0$ . But interestingly at  $2R = 0.2\text{mm}$ , the curve has a dip at  $x = 0$  and the  $S_{21\text{max}}$  deviates from the center of the gap.

#### 3.2 Wide Band Transmission Characteristics under Laser Illumination

Figure 4 shows the relationship between the transmission characteristics  $S_{21}$  and the plasma density at the frequencies of 5GHz and 10GHz. Laser spot is focused at the center of the gap. In particular, it is noted that the  $S_{21}$  varies with the frequency at the low density of plasma, but when the plasma density is more than  $10^{21} / \text{m}^3$ , the  $S_{21}$  shows no dependency on the frequency characteristic.

To show this feature clearly, the frequency characteristics of  $S_{21}$  are presented in figure 5 with the plasma density as a parameter. These results indicate that the illumination of laser spot develops the non-dispersive characteristics of  $S_{21}$  for the wide frequency range. The performance of wide frequency range, from DC to nearly 30GHz, can be attained at the plasma density of  $n_p = 10^{22} / \text{m}^3$ . This phenomenon can be successfully applied to generate millimeter waves using a dc-biased microstrip gap aided with transient from picosecond optical pulse.

### 4. Experiment

#### 4.1 Experimental Setup

Experiments have been carried out at the frequency

range from 6 to 9GHz using an arrangement as shown in figure 6<sup>[7]</sup>. We have fabricated a microstrip line on a silicon substrate with high resistivity of about  $5000\Omega \cdot \text{cm}$  and thickness  $h = 0.4\text{mm}$ . The strip with  $w = 1.0\text{mm}$  containing a gap with  $G_w = 0.5\text{mm}$  was made by evaporating aluminum. The silicon surface around the gap was illuminated by a semiconductor laser with the wavelength of 870nm, the optical power of 10mW and the diameter of laser spot of approximately 0.01mm. The laser was mounted on the manipulator so that the laser spot can scan in X and Y directions. The lock-in amplifier was synchronized with the laser power modulated at 1000Hz.

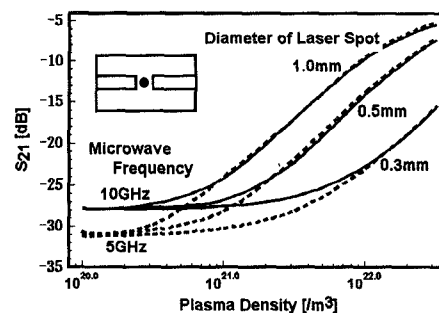


Fig.4 Relationship between the  $S_{21}$  and the plasma density.

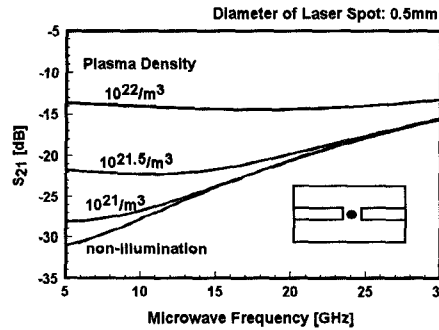


Fig.5 Frequency characteristics of  $S_{21}$  with the plasma density as a parameter.

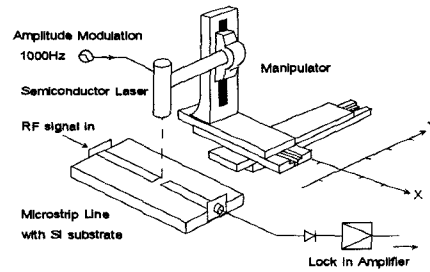


Fig.6 Experimental Setup.

#### 4.2 Experimental Results

To compare the theoretical results with the experimental ones, the transmission characteristic  $S_{21}$  was measured when the laser spot scanned around the gap.

Figure 7 shows the relationship between the  $S_{21}$  and the position of laser spot on Y-axis with the microwave frequency as a parameter. It is clear from the graph that the maximum value of  $S_{21}$  is obtained for all of curves when the laser spot is focused at the center of the gap. These results correspond to those in figure 2.

Figure 8 shows the value of  $S_{21}$  at the different point on X-axis. The microwave frequency is fixed at 9.0GHz. In this case, as the diameter of laser spot used here is sufficiently small comparing with the gap width, the dip of  $S_{21}$  can be observed at  $x = 0$ , which is suggested theoretically in figure 3.

Even though the experimental parameters and the theoretical parameters have different numerical values, they are phenomenologically agreed with.

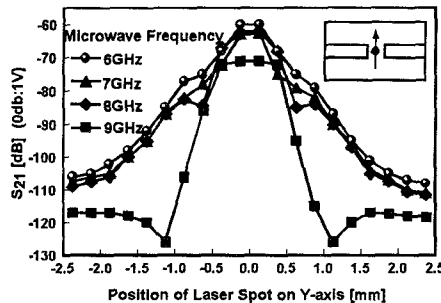


Fig.7 The measured  $S_{21}$  when the laser passes through Y-axis.

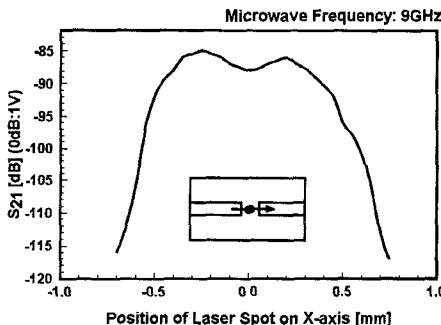


Fig.8 The measured  $S_{21}$  when the laser passes through X-axis.

#### 5. Conclusion

We have demonstrated in detail the transmission characteristics  $S_{21}$  of the microstrip line containing an optically controlled microstrip gap both theoretically and experimentally at the frequency range from C to X band. We have confirmed that the measured  $S_{21}$  when the laser spot scans around the gap, had the similar properties with the theoretical one.

Further, we have calculated the frequency characteristics of  $S_{21}$  with the plasma density and reported that the high-powered illumination of laser spot developed the non-dispersive characteristics of  $S_{21}$  for the wide frequency range.

#### Acknowledgment

The authors wish to acknowledge to Dr. H.Shimasaki from Kyoto Institute of Technology for his kind and useful discussion on this work.

This research has been supported by "Special Research Fond of Kansai University".

#### References

- [1] C.H.Lee, P.S.Mak, A.P.DeFonzo: "Optical control of millimeter-wave propagation in dielectric waveguides", IEEE Quantum Electron., QE-16, 3, pp.277-288, March 1980.
- [2] Y.Horii, M.Tsutsumi: "Scattering parameter of microstrip line with semiconductor substrate under laser illumination", Technical Report of IEICE Japan, MW95-16, pp.37-42, May 1995.
- [3] R.Luebbers, F.Hunsberger, K.Kunz, R.Standler, M.Schneider: "A frequency-dependent finite-difference time-domain formulation for dispersive materials", IEEE Trans., Electromagn. Compat., vol.32, pp.222-227, Aug. 1990.
- [4] R.Luebbers, F.Hunsberger, K.Kunz: "A frequency-dependent finite-difference time-domain formulation for transient propagation in plasma", IEEE Trans. on Ant. and Prop., AP-39, pp.29-34, Jan. 1991.
- [5] K.S.Yee: "Numerical solution of initial boundary value problems involving Maxwell's equations in isotropic media", IEEE Trans. on Ant. and Prop., AP-14, 5, pp.302-307, May 1966.
- [6] G.Mur: "Absorbing boundary conditions for finite-difference approximation of the time-domain electromagnetic-field equations", IEEE Trans., Electromagn. Compat., EMC-23, pp.1073-1077, Nov. 1981.
- [7] A.Alphones, M.Tsutsumi: "Optical probing of millimeter waves in semiconductor waveguides", IEE Proc.-H, vol.138, no.5, pp.460-462, Oct. 1991.